

# Transition States and Mechanisms of the Hetero-Diels–Alder Reactions of Hyponitrous Acid, Nitrosoalkanes, Nitrosoarenes, and Nitrosocarbonyl Compounds

Andrew G. Leach and K. N. Houk\*

Department of Chemistry and Biochemistry, University of California, Los Angeles, California 90095-1569

houk@chem.ucla.edu

Received April 23, 2001

The transition states and energetics of Diels–Alder reactions for a variety of nitroso compounds with dienes were explored with density functional theory using the B3LYP functional and 6-31G\* basis set. The reactions involve HNO, various nitrosoalkanes and arenes (RNO and ArNO), and nitrosoformaldehyde (CHONO) as dienophiles with butadiene and a series of 1- and 2-substituted dienes. The mechanisms, activation energies, energies of reaction, stereoselectivities, and regioselectivities are predicted for these reactions. These predictions are compared to available experimental data. The mechanism is found to be concerted but involves highly asynchronous transition states. Although it is not evident in the products, we find that the endo path is very strongly favored over the exo alternative due to repulsion between the diene and nitrogen's lone pair. A range of experimental regioselectivities are reproduced by calculations and are found to hinge on a very sensitive balance between FMO interactions, electrostatics, and steric effects. A series of generalizations for predicting regioselectivity for untried diene–dienophile pairs are made.

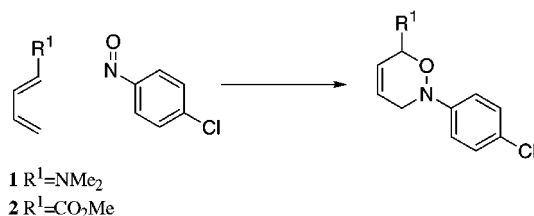
## Introduction

Since the first hetero-Diels–Alder reaction of a nitroso compound was reported by Wichterle in 1947,<sup>1</sup> much attention has focused on the generality, mechanism, and applications of these reactions in synthesis. Nitroso compounds are very reactive dienophiles, but they exhibit unpredictable regioselectivities. Kresze and Firl found that dienes **1** and **2**, which possess electron-donating and electron-withdrawing substituents, respectively, both give the same regioisomer with *p*-chloronitrosobenzene (Scheme 1).<sup>2</sup>

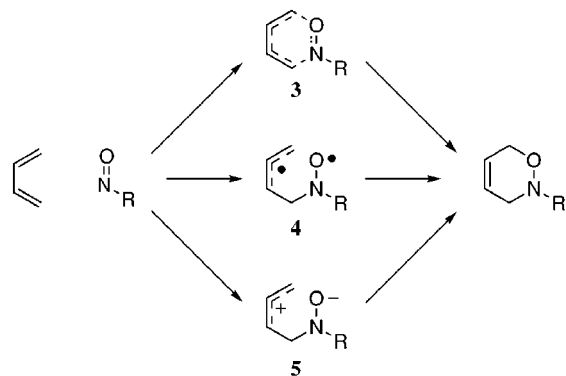
A number of possibilities may be proposed for the mechanistic pathway that is followed by these reactions. The simplest and most commonly proposed mechanism is a concerted [4 + 2]-cycloaddition, or Diels–Alder reaction, proceeding through a transition state such as **3**. There are, however, two alternative stepwise mechanisms: one proceeding through a diradical intermediate such as **4**, the other preferring a zwitterionic intermediate such as **5**. Both of these stepwise pathways have some attractive features. The diradical path involves a nitroxyl and allylic radical containing intermediate **4**. Both of these are known to be stabilized radical types, and this stabilization may be reflected in a low energy intermediate. Similarly, the zwitterionic path involves an intermediate **5** with an allylic cation and a nitroxylate anion; again, these might be expected to be energetically attractive features (Scheme 2).

An ongoing interest in understanding and improving catalysis by designer antibodies provides further impetus for these studies. An antibody to catalyze the hetero-Diels–Alder reaction of **6** has been reported by Meekel

## Scheme 1 Outcome of the Hetero-Diels–Alder Reactions of an Electron-Rich and an Electron-Deficient Diene



## Scheme 2. Possible Mechanisms for the Hetero-Diels–Alder Reaction of Nitroso Compound RNO with Butadiene

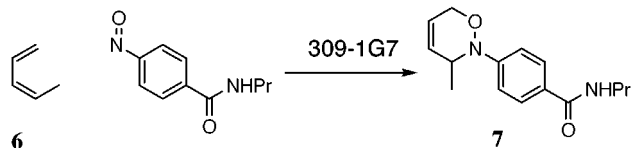


et al., and the adduct **7** could be obtained with greater than 82% ee (Scheme 3).<sup>3</sup> Similarly, Reymond and Lerner have disclosed that antibody 9D9 catalyzes the retro-Diels–Alder reaction of **8** but not its regioisomer (Scheme 4).<sup>4</sup> They also showed that the HNO liberated in this

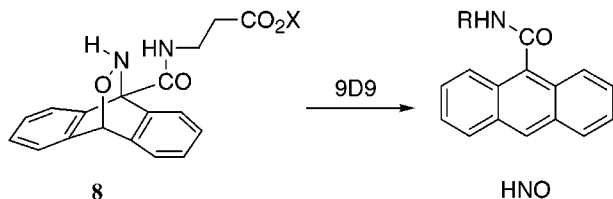
(1) Wichterle, O. *Collect. Czech. Chem. Commun.* **1947**, *12*, 292–304.

(2) Kresze, G.; Firl, J. *Tetrahedron Lett.* **1965**, 1163–1170.

(3) (a) Meekel, A. A. P.; Resmini, M.; Pandit, U. K. *J. Chem. Soc., Chem. Commun.* **1995**, 571–572. (b) Resmini, M.; Meekel, A. A. P.; Pandit, U. K. *Pure and Appl. Chem.* **1996**, *68*, 2025–2028.

**Scheme 3. Diels–Alder Reaction Catalyzed by Antibody 309-1G7<sup>a</sup>**

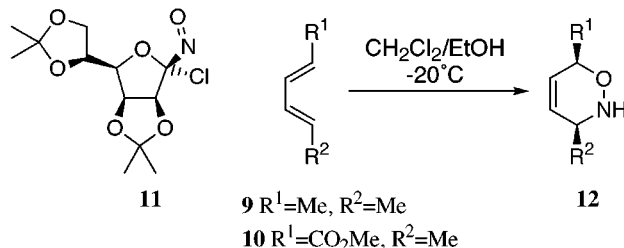
<sup>a</sup> Adduct 7 is obtained with 82% ee.

**Scheme 4. Retro-Diels–Alder Reaction Catalyzed by Antibody 9D9**

reaction is oxidized by the bio-oxidant superoxide dismutase to the important signaling molecule NO. It has recently been found that HNO may itself be a biologically relevant species.<sup>5</sup> If these antibody systems are to be improved upon, better hapten molecules that mimic the transition state will be required. Designing such molecules requires a detailed knowledge of the structure and electronic characteristics of the transition states for these reactions.

A key expectation from any proposed mechanism and calculations is that they should be able to explain the regiochemical outcomes of the reactions of nitroso compounds with substituted dienes. A number of authors have proposed methods for predicting these regioselectivities with greater or lesser degrees of success. For instance, Eisenstein et al. compared the predictive capabilities of Hückel and CNDO/2 methods for the regioselectivity of Diels–Alder reactions of *p*-chloronitrosobenzene.<sup>6</sup> They found both to be severely lacking and attributed this to critical interactions involving the lone pairs of the nitroso species being neglected. Interestingly, they did not speculate as to the nature of these interactions or on the form of the transition state for these reactions. Kresze proposed the nature of the transition states for this class of reactions based on a number of experimentally observed regioselectivities.<sup>7</sup> He suggested that it will be intermediate between a nonpolar concerted structure and a highly polar structure closely resembling a zwitterionic intermediate, dependent upon the exact nature of the reactants. Boger proposed that the regiochemical outcomes for 1- and 2-substituted butadienes might be governed by steric effects but found this surprising as he felt that “such effects must be relatively removed from the reaction centers”.<sup>8</sup>

A final, but crucial, facet of these reactions that we hoped to address was their stereoselectivity. The most

**Scheme 5. Asymmetric Hetero-Diels–Alder Reaction of Sugar Derived Dienophiles<sup>a</sup>**

<sup>a</sup> Adduct 12 is obtained by in situ solvolysis and is obtained with ee greater than 96%.

obvious aspect of this would be to explain and understand the high selectivities observed by Vasella and others who found that the cycloaddition of 9 or 10 with 11 allowed access to a range of synthetically useful species such as 12 with very high enantiomeric excesses (>96%) (Scheme 5).<sup>9</sup> Indeed, very recently, Royer et al. have reported a synthesis of the potent analgesic (–)-epibatidine in which the source of chirality is a similar asymmetric Diels–Alder reaction of a nitroso dienophile.<sup>10</sup>

There is, however, a further aspect of stereoselectivity that is not apparent in the product of these reactions because of rapid inversion at nitrogen. There are two possible pathways, with the substituent on nitrogen either exo or endo in the transition state. Hartree–Fock calculations from this group have shown that several heterodienophiles have a surprisingly large preference for the endo transition state.<sup>11</sup> This “exo-lone-pair effect” was attributed to repulsive electrostatic interactions between the lone pairs of the dienophile and the  $\pi$ -electrons of the diene. Although this selectivity does not manifest itself in the product of the reaction, it may have important implications for their regio- and stereochemical outcomes.

**Computational Methods**

All calculations were performed with GAUSSIAN 98.<sup>12</sup> Most structures were optimized with the B3LYP functional<sup>13</sup> and the 6-31G\* basis set.<sup>14</sup> Some structures were optimized with

(9) Felber, H.; Kresze, G.; Prewo, R.; Vasella, A. *Helv. Chim. Acta* **1986**, *69*, 1137–1146.

(10) (a) Cabanal-Duvillard, I.; Berrien, J.-F.; Ghosez, L.; Husson, H.-P.; Royer, J. *Tetrahedron* **2000**, *56*, 3763–3769. (b) Cabanal-Duvillard, I.; Berrien, J.-F.; Royer, J. *Tetrahedron: Asymmetry* **2000**, *11*, 2525–2529.

(11) (a) McCarrick, M. A.; Wu, Y.-D.; Houk, K. N. *J. Am. Chem. Soc.* **1992**, *114*, 1499–1500. (b) McCarrick, M. A.; Wu, Y.-D.; Houk, K. N. *J. Org. Chem.* **1993**, *58*, 3330–3343.

(12) Gaussian 98 (Revision A.7): Frisch, M. J.; Trucks, G. W.; Schlegel, H. B.; Scuseria, G. E.; Robb, M. A.; Cheeseman, J. R.; Zakrzewski, V. G.; Montgomery, J. A.; Stratmann, R. E.; Burant, J. C.; Dapprich, S.; Millam, J. M.; Daniels, A. D.; Kudin, K. N.; Strain, M. C.; Farkas, O.; Tomasi, J.; Barone, V.; Cossi, M.; Cammi, R.; Mennucci, B.; Pomelli, C.; Adamo, C.; Clifford, S.; Ochterski, J.; Petersson, G. A.; Ayala, P. Y.; Cui, Q.; Morokuma, K.; Malick, D. K.; Rabuck, A. D.; Raghavachari, K.; Foresman, J. B.; Cioslowski, J.; Ortiz, J. V.; Stefanov, B. B.; Liu, G.; Liashenko, A.; Piskorz, P.; Komaromi, I.; Gomperts, R.; Martin, R. L.; Fox, D. J.; Keith, T.; Al-Laham, M. A.; Peng, C. Y.; Nanayakkara, A.; Gonzalez, C.; Challacombe, M.; Gill, P. M. W.; Johnson, B. G.; Chen, W.; Wong, M. W.; Andres, J. L.; Head-Gordon, M.; Replogle, E. S.; Pople, J. A. Gaussian, Inc., Pittsburgh, PA, 1998.

(13) A combination of Becke's three parameter exchange functional and Lee, Yang and Parr's correlation functional: Becke, A. D. *J. Chem. Phys.* **1993**, *98*, 5648–5652. Lee, C.; Yang, W.; Parr, R. G. *Phys. Rev. B* **1988**, *37*, 785–789.

(14) Hariharan, P. C.; Pople, J. A. *Theo. Chem. Acta* **1973**, *28*, 213–222.

(4) Bahr, N.; Güller, R.; Reymond, J.-L.; Lerner, R. A. *J. Am. Chem. Soc.* **1996**, *118*, 3550–3555.

(5) Bartberger, M. D.; Fukuto, J. M.; Houk, K. N. *Proc. Natl. Acad. Sci. U.S.A.* **2001**, *98*, 2194–2198.

(6) Eisenstein, O.; Lefour, J. M.; Anh, N. T.; Hudson, R. F. *Tetrahedron* **1977**, *33*, 523–531.

(7) (a) Kresze, G.; Kosbahn, W. *Tetrahedron* **1971**, *27*, 1931–1939. (b) Kresze, G.; Saitner, H.; Firl, J.; Kosbahn, W. *Tetrahedron* **1971**, *27*, 1941–1950.

(8) Boger, D. L.; Patel, M.; Takusagawa, F. *J. Org. Chem.* **1985**, *50*, 1911–1916.

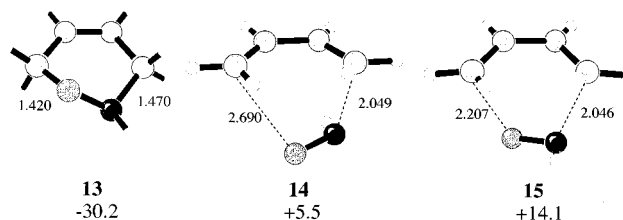


**Figure 1.** B3LYP/6-31G\* geometries for the product and two concerted transition states for HNO + butadiene.

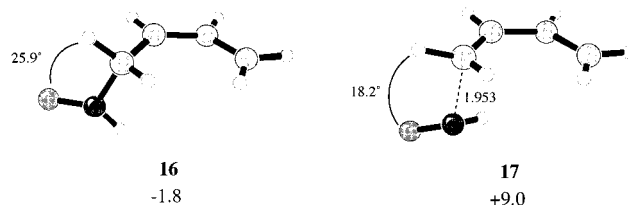


**Figure 2.** Singlet diradical intermediate for the stepwise Diels–Alder reaction of HNO with butadiene and the rate-limiting transition state linking it to reactants.

MP2 and the 6-31G\* basis set. Diradicals and transition states leading to diradicals were treated with unrestricted B3LYP; HOMO–LUMO mixing in the initial guess led to unrestricted wave functions when these were more stable than restricted wave functions. All minima and transition states were characterized by their vibrational frequencies. Unless otherwise indicated, all energy changes reported in this paper include zero-point energies, which are included without scaling. Intrinsic reaction coordinate searches (IRC) were performed in a few representative cases. Constrained minimizations were performed using redundant coordinates in GAUSSIAN 98.

## Results and Discussion

**1. Mechanism: Concerted or Stepwise?** Using B3LYP/6-31G\*, we have mapped out the important points on the potential energy surface for the reaction of a range of nitroso compounds (RNO) with butadiene and for HNO with other substituted dienes. To establish the nature of the mechanism of these hetero-Diels–Alder reactions, the reaction of HNO with butadiene was studied in detail.

Having obtained the structures of HNO, butadiene, and the cycloaddition product **13** with B3LYP/6-31G\*, an overall energy change for this reaction of  $-30.2$  kcal/mol was calculated. Furthermore, a number of transition states and possible intermediates have been identified. Two transition states similar to those expected for a concerted pathway were identified. One has the NH bond endo (**14**) and the other exo (**15**) (Figure 1). Transition state **14** is exceedingly asynchronous and has an activation barrier of only  $5.5$  kcal/mol. The exo transition state **15** is more nearly synchronous and has an activation barrier of  $14.1$  kcal/mol.

We were also able to identify the singlet diradical **16** and the transition state linking it to reactants, **17**. Although **16** is  $1.8$  kcal/mol lower in energy than the reactants, **17** is  $9.0$  kcal/mol above reactants. A series of restricted optimizations linking diradical **16** to the Diels–Alder product, by variation of the ONCH dihedral angle, showed that there is a barrier of approximately  $2.7$  kcal/mol for formation of the second bond. The rate-determining step of this stepwise path is formation of the diradical. There is a higher barrier ( $\sim 3.3$  kcal/mol) to rotation about the CN bond in the opposite direction. The diradical has

**Table 1.** Computed Activation Energies (in kcal/mol) at Varying Levels of Theory for the Reaction of HNO with Butadiene

theory	$\Delta H^\ddagger(\text{endo})$	$\Delta H^\ddagger(\text{exo})$	$\Delta\Delta H^\ddagger$
RHF/3-21G//RHF/3-21G	23.6	31.0	7.4
MP2/6-31G**//RHF/3-21G	1.8	9.9	8.1
RB3LYP/6-31G**//RB3LYP/6-31G*	5.5	14.1	8.6
MP2/6-31G**//MP2/6-31G*	3.1	12.7	9.6

only one conformational energy minimum, shown in **16**. This conformation keeps the electron density due to the lone pairs on N and O away from the  $\pi$  electron density of the allyl radical. Our studies with substituted nitroso compounds (Table 4) and substituted dienes (Table 7) show that, in all cases, the concerted endo transition state is lowest in energy, the stepwise transition state like **17**, linking reactants to a diradical is next, and the exo transition state is highest in energy. In the case of the most favorably substituted diene (*cis*-1-CN-substituted butadiene), with HNO, in which all factors are stacked in favor of the stepwise reaction, the stepwise transition state is only  $1.2$  kcal/mol above the concerted endo transition state. The stepwise path passing through a diradical exists for this Diels–Alder reaction and may come close enough in energy to make an observable contribution to the product mixture in some cases.

As indicated in Figure 1, the C–N to C–O bond length ratio in the product is 1:0.97, whereas in **14** it is 1:1.3 and in **15** 1:1.1. It seemed possible therefore that **14** may actually link the starting materials to an intermediate in which the C–N bond is fully formed but with negligible formation of the C–O bond. It is noteworthy that the C–O separation of  $2.69$  Å in **14** is closer to the sum of the van der Waals' radii for C and O ( $3.25$  Å) than it is to the length of the final C–O bond ( $1.42$  Å). A series of constrained minimizations linking the transition states to the products was performed with both B3LYP/6-31G\* (restricted and unrestricted) and MP2/6-31G\*. They showed that the transition state is followed by a very flat area of the potential energy surface before the well leading down to the products. There is no intermediate between the transition state and the products. Furthermore, this flat region may lead one to suggest that a synchronous structure would be rather close in energy to the actual transition state. The exo and endo transition states already obtained were constrained to be synchronous and reoptimized. It was found that in the endo case this cost  $2.0$  kcal/mol, whereas in the exo case a disadvantage of only  $0.3$  kcal/mol was observed. The very flat area around the transition state found for HNO with butadiene suggests that changing substituents may shift the transition state to a more or less synchronous structure without significantly changing its energy and without making the mechanism stepwise. This concurs with Kresze's suggestion<sup>2</sup> that the transition state can be shifted between a highly polar one and a nonpolar one by changing the substituents on the diene or dienophile.

The transition states **14** and **15** are similar to those obtained using the RHF/3-21G method described by McCarrick, Wu, and Houk.<sup>11</sup> These structures had been used to perform single-point energy calculations at the MP2/6-31G\* level. The values they obtained for the activation energies and the difference in activation energies are shown in Table 1 alongside the corresponding energies with B3LYP/6-31G\*\*//B3LYP/6-31G\* and MP2/6-31G\*\*//MP2/6-31G\* obtained during the course of our studies. While the absolute barriers had been over-



**Table 2. Asynchronicities ( $I_{\text{CN}}^{\text{TS}}$ ,  $I_{\text{CO}}^{\text{Prod}}$ ,  $I_{\text{CO}}^{\text{TS}}$ ,  $I_{\text{CN}}^{\text{Prod}}$ ) for the Endo and Exo Transition States of the RNO + Butadiene Reaction**

R	asynchronicity (endo path)	asynchronicity (exo path)
H	1.61	1.32
Me	1.41	1.20
Et	1.42	1.18
<i>i</i> -Pr	1.40	1.16
<i>t</i> -Bu	1.48	1.36
Ph	1.38	1.09
CHO ( <i>s</i> -trans)	1.29	0.83
CHO ( <i>s</i> -cis)	1.22	1.09

estimated by RHF and underestimated by MP2, the differences in energy between exo and endo transition states are remarkably constant. B3LYP and MP2 agree upon the barriers to a sufficient degree. Although it would be desirable to compare these or other calculated values to experimentally determined activation barriers, these are hard to obtain and unreliable due to the many side reactions (such as dimerization) undergone by these highly reactive dienophiles.

We have identified the transition states for the reactions of a range of nitroso compounds, RNO, with butadiene for R = H, Me, Et, *i*-Pr, *t*-Bu, Ph, and CHO (reacting in both its *s*-cis and *s*-trans conformations) using B3LYP calculations. These transition states resemble very closely those already discussed for HNO. We assessed the asynchronicity of the concerted transition states for all of these reactions by comparing the ratio of the C–N distance to the C–O distance in the transition state to the same ratio in the product of the reaction. As these values (Table 2) show, the favored endo transition state is always much more asynchronous than its exo counterpart.

Interestingly, the most asynchronous path is that already discussed (HNO) and the least is for the highly reactive CHONO. We conclude therefore that our proposed mechanism for HNO is valid for other nitroso compounds and that the reactions of HNO, nitrosoalkanes, nitrosoarenes, and nitrosocarbonyl compounds with simple dienes are highly asynchronous but nevertheless concerted cycloadditions.

The asynchronicity of these concerted reactions might arise from the asymmetry of the dienophile, both in the sense of the polar N–O grouping and in that the nitroso compound presents two lone pairs (on N and O) to the diene in the exo transition state but only one (on O) in the endo. While this is certainly a major factor, asynchronous transition states have even been observed in the Diels–Alder reactions of symmetric triazolinediones.<sup>15</sup> Asynchronicity seems to be a feature of potentially synchronous reactions, which have very low barriers to reaction. Moreover, in their studies of the Diels–Alder reaction of <sup>1</sup>O<sub>2</sub>, Bobrowski et al. attribute the second-order nature of the synchronous transition state with butadiene to the fact that in the product the conformation that has this arrangement is a transition state linking two pseudo-chair conformations,<sup>16</sup> and this is the case here as well.

We also explored polar effects in these transition states. Kresze proposed that the transition state has a structure that is intermediate between nonpolar and

**Table 3. Charge Transfer from the Diene to the Nitroso Compound and Dipole Moments of the Endo Transition States for the RNO + Butadiene Reaction**

R	charge transfer/e <sup>-</sup> (endo path)	dipole moment/D (endo TS)
H	0.13	2.10
Me	0.14	2.05
Et	0.13	2.00
<i>i</i> -Pr	0.15	1.97
<i>t</i> -Bu	0.12	2.00
Ph	0.15	2.24
CHO ( <i>s</i> -trans)	0.22	2.49

zwitterionic.<sup>7</sup> Significant charge transfer of 0.1–0.2 electrons from diene to dienophile is observed in the transition states located here; the dipole moments of the transition states range from 2 to 2.5 D (Table 3). For comparison, the nitroso compound reactants have dipole moments of 1.6 (HNO)–3.8 (PhNO) D. These reactions are therefore expected to be somewhat sensitive to solvent polarity and to varying degrees.

The stepwise transition states were found to have a smaller dipole moment than the corresponding endo transition states with the exception of that for PhNO. The usual favoring of open stepwise transition states by polar solvents is not expected to operate here. The endo transition state is expected to be dominant even in polar solvents.

**2. Endo versus Exo Selectivity in the Concerted Pathway.** Although the reaction of HNO with butadiene strongly favors the pathway that has the substituent on nitrogen endo, substituents that are more sterically demanding might affect the degree to which this was the case and may even favor the stepwise or exo path. The transition states so far described allowed an assessment of this to be made. The activation barriers and energies of reaction are given in Table 4.

The activation energy for all three pathways is found to be more or less directly proportional to the energy change for the reaction, suggesting that the effect of varying R in RNO on the stability of the product also influences the transition-state energy. The highly reactive formylnitroso compound has a low activation energy but is even more exothermic than expected from its  $\Delta H^\ddagger$ . This reaction is anomalously exothermic because the final product is an amide rather than an amine. The amide resonance stabilization cannot operate fully in the transition state, where the lone pair is nearly orthogonal to the carbonyl  $\pi$  orbital.

Strikingly, the large difference in energy between the endo and the exo pathways is maintained in all cases, even for the very bulky *t*-BuNO and for the highly exothermic reaction of nitrosoformaldehyde. This latter reaction may proceed through four possible transition states: two (endo and exo) with the CHONO in an *s*-trans arrangement and two for the corresponding *s*-cis arrangement. It was found that for both endo and exo cases that the *s*-trans arrangement that minimizes the dipole moment of the transition state was favored. The second lowest *s*-cis endo transition state is only 1.3 kcal/mol higher in energy than its *s*-trans counterpart. This ordering may be different with COR because in the *s*-trans arrangement the R group would interact sterically with the diene and with the nitroxyl oxygen.

The strong preference for an endo path is believed to arise from an unfavorable interaction between the nitrogen lone pair with the  $\pi$  electrons of the electron-rich

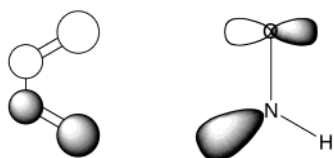
(15) Chen, J. S.; Houk, K. N.; Foote, C. S. *J. Am. Chem. Soc.* **1998**, *120*, 12303–12309.

**Table 4. B3LYP/6-31G\* Activation Enthalpies and Enthalpies of Reaction (in kcal/mol) for RNO + Butadiene**

R	$\Delta H^\ddagger$ (endo)	$\Delta H^\ddagger$ (exo)	$\Delta\Delta H^\ddagger$ (exo-endo)	$\Delta H^\ddagger$ (stepwise)	$\Delta\Delta H^\ddagger$	$\Delta H$
H	5.5	14.1	8.6	9.0	3.5	-30.2
Me	11.6	18.3	6.7	17.1	5.4	-26.0
Et	13.4	20.8	7.5	18.7	5.4	-24.3
<i>i</i> -Pr	14.6	21.4	6.8	18.3	3.7	-22.7
<i>t</i> -Bu	13.2	20.5	7.3	20.0	6.7	-23.3
Ph	14.4	20.3	5.9	20.2	5.8	-21.1
CHO ( <i>s</i> -trans)	3.6	10.0	6.4	8.1	4.5	-45.1
CHO ( <i>s</i> -cis)	4.9	10.6	5.7	10.1	5.2	-45.1

**Table 5. B3LYP/6-31G\* Activation Energies (in kcal/mol) for the Endo Reactions of HNO and CHONO with Substituted Dienes**

entry	substituent on diene	HNO			CHONO		
		$\Delta H^\ddagger$ (proximal)	$\Delta H^\ddagger$ (distal)	$\Delta\Delta H^\ddagger$ (d-p)	$\Delta H^\ddagger$ (proximal)	$\Delta H^\ddagger$ (distal)	$\Delta\Delta H^\ddagger$ (d-p)
1	<i>trans</i> -1-MeO	3.2	4.1	0.9	0.1	4.1	4.1
2	<i>trans</i> -1-Me	4.8	5.4	0.6	2.4	2.7	0.3
3	<i>trans</i> -1-CN	5.5	9.8	4.3	4.8	10.0	5.3
4	2-MeO	5.8	5.9	0.1	3.7	1.0	-2.7
5	2-Me	5.4	5.5	0.1	3.3	2.5	-0.8
6	2-CN	5.5	4.2	-1.3	4.9	4.4	-0.5
7	<i>cis</i> -1-MeO	4.9	4.8	-0.1			
8	<i>cis</i> -1-Me	8.8	7.0	-1.8			
9	<i>cis</i> -1-CN	8.2	12.6	4.4			

**Figure 3.** HOMOs of HNO and butadiene.

diene in the exo transition state. Previously, this “exo lone pair effect”, that is, the lone pair’s preference to be exo, has been ascribed to mainly a strong electrostatic repulsion between the nitrogen lone pair and the diene  $\pi$  electrons.<sup>11</sup> An alternative but complementary rationalization for this effect can be obtained by considering FMO interactions. In the standard Diels–Alder reaction, the HOMO(diene)–HOMO(dienophile) interaction is symmetry forbidden. However, the HOMO of a nitroso dienophile is the antibonding combination of N and O lone pairs (Figure 3). This has the correct symmetry to overlap in a four-electron repulsive fashion with the HOMO of the diene. This is minimized in the endo path.

The preference for an endo path supports Boger’s tentative proposal that steric effects are important in governing regioselectivity.<sup>8</sup> The nitrogen substituent is not far removed from the reactive centers as he expected; in fact, the substituent on nitrogen is held in close proximity to the diene component by the exo lone pair effect.

**3. Regioselectivity.** Using the methodology already described, the transition states for the cycloaddition reactions of HNO and CHONO with butadienes bearing methoxyl, methyl, or nitrile substituents at both the 1 and 2 positions were obtained. For 1-substituted dienes, both *cis* and *trans* reactants and transition states are possible, and both were investigated. All of these examples were found to preferentially follow the highly asynchronous concerted endo pathway delineated for HNO with butadiene.

The activation energies for each process enabled an assessment of regioselectivity (Table 5). We first established that product stability is unrelated to regioselectivity. The energies of reaction for reactions of HNO with various dienes were obtained (Table 6). A plot of activa-

**Table 6. B3LYP/6-31G\* Reaction Energies (in kcal/mol) for the Reactions of HNO with Substituted Dienes**

entry	substituent	$\Delta H$ (proximal)	$\Delta H$ (distal)
1	<i>trans</i> -1-MeO	-25.0	-29.9
2	<i>trans</i> -1-Me	-29.9	-28.8
3	<i>trans</i> -1-CN	-21.9	-22.3
4	2-MeO	-26.5	-26.7
5	2-Me	-31.9	-31.8
6	2-CN	-32.7	-32.6
7	<i>cis</i> -1-MeO	-31.2	-26.3
8	<i>cis</i> -1-Me	-31.6	-30.5
9	<i>cis</i> -1-CN	-22.2	-22.6

tion energy versus energy of reaction showed no correlation. In several cases, the more stable regioisomer is formed by the path with the highest activation energy. For all of these reactions, the forming C–N distances are 1.92–2.14 Å while the C–O distances are 2.49–2.85 Å.

The stepwise and exo transition states were also obtained for each of the reactions with HNO. These were found to be disfavored, as expected, but the stepwise path is competitive for reactions with 1-CN-substituted dienes, and the relative energies of endo to exo transition states for each regioisomer provided information about the origins of regioselectivity (Table 7).

Scheme 6 summarizes the reactions that were studied. The nomenclature employed to describe the regiochemistry is the same as that used by Boger.<sup>8</sup> The proximal isomer is the one in which the diene substituent is closest to the oxygen and the distal is that in which the substituent is furthest from oxygen.

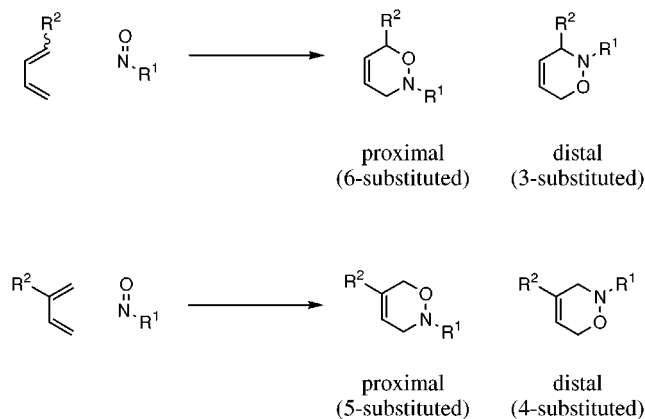
Experimentally observed regioselectivities are summarized in Table 8 and will be used to illustrate the discussion of our data.

A detailed analysis of the factors leading to the regioselectivity calculated for each of the substituted dienes demonstrated that these include three important FMO interactions. The principal interaction is between HOMO(diene) and LUMO(dienophile). For all the 1-substituted dienes studied, the HOMO should have its largest coefficient at the 4-position.<sup>22</sup> This should there-

(16) Bobrowski, M.; Liwo, A.; Oldziej, S.; Jeziorek, D.; Ossowski, T. *J. Am. Chem. Soc.* **2000**, *122*, 8112–8119.

**Table 7. Activation Energies for the Stepwise and Exo (Disfavored) Transition States for HNO with Substituted Dienes (in kcal/mol)**

entry	substituent	stepwise		exo	
		$\Delta H^\ddagger$ (proximal)	$\Delta H^\ddagger$ (distal)	$\Delta H^\ddagger$ (proximal)	$\Delta H^\ddagger$ (distal)
1	<i>trans</i> -1-MeO	9.9	13.3	10.5	14.7
2	<i>trans</i> -1-Me	9.9	9.8	13.0	14.3
3	<i>trans</i> -1-CN	9.1	15.1	14.5	17.1
4	2-MeO	9.9	9.6	15.4	14.1
5	2-Me	9.8	6.8	14.0	13.4
6	2-CN	9.7	8.0	14.2	10.9
7	<i>cis</i> -1-MeO	8.6	8.5		
8	<i>cis</i> -1-Me	11.7	10.4		
9	<i>cis</i> -1-CN	9.4	15.0		

**Scheme 6. Regiochemistries of Diels–Alder Reactions of Nitrosoalkanes with Substituted Dienes**

fore favor the proximal adduct because the LUMO of RNO (the NO  $\pi^*$  orbital) is largest at nitrogen. Electron-donating (D) substituents should be most influential in this way, conjugating substituents (C) next and electron-withdrawing (Z) substituents least. Similarly, the 2-substituted dienes should have their largest HOMO coefficients at C-1, and hence, the distal isomer is expected. The importance of this interaction is also reflected in the shortened C–N bond.

When acceptor substituents (Z) on the diene lower the energy of its LUMO, the interaction between this orbital and the RNO HOMO (dominated by the nitrogen lone pair) gains in significance. This further favors the proximal isomer for 1- and the distal isomer for 2-Z-substituted dienes. Interaction between the two HOMOs may also contribute but this is less significant than in the exo transition states.

Secondary interactions involving components of each of these orbitals on the nitroso and diene substituents perturb these simple interactions and particularly contribute to the high selectivity for 1-substituted dienes.<sup>23</sup> This arises principally because the HOMO of the diene includes an antibonding interaction with orbitals on the substituent (Figure 4).

Electrostatics also play a key part in this selectivity, the partial charges on the primary atoms involved in bond formation must be supplemented by those on the substituents to gain a full insight. This is particularly true for the 1-*cis*-substituted dienes where an intimate interaction occurs between the diene substituent and the N or O of RNO. The complex balancing of these factors prevents us from painting a simple predictive picture. Instead, the calculated energetics allow us to make general conclusions about the net directing effect of a range of substituent types in these reactions.

To test whether the directing effects of substituents may be considered together, the experimentally known reaction of *p*-chloronitrosobenzene with butadiene bearing 1-CN and 4-Me substituents (**18**) was studied. This reaction is known to give only isomer **19** (Scheme 7).<sup>2</sup>

Our calculations using HNO as a model dienophile showed an activation barrier of 4.2 kcal/mol to form the HNO adduct analogous to **19** and 7.7 kcal/mol for its regioisomer. The nitrile substituent alone favors **19** by 4.3 kcal/mol and the methyl substituent would disfavor it by 0.6 kcal/mol (Table 5). Adding these effects confers a preference for **19** of 3.7 kcal/mol—in very good agreement with the actual value of 3.6 kcal/mol.

Our results compare well to experiment, as shown by comparison of Table 5 to Table 8. We can make the following generalizations:

(1) *Trans*-1-substituted dienes all favor the proximal isomer in accord with the FMO prediction and results of computations; see Table 5, entries 1–3, and Table 8, entries 1–6.

(2) Selectivity for 1-substituted dienes is generally higher than for the corresponding 2-substituted dienes; see Table 5, entries 4–6, and Table 8, entries 9–16, compare to Table 5, entries 1–3, and Table 8, entries 1–6. This is in accord with other Diels–Alder reactions and arises from the fact that the substituent  $\pi$  MO interacts in an antibonding fashion with the 1-position of the diene.

(3) The direction of selectivity in the case of 2-substituted dienes is sensitive to the nature of the dienophile; see Table 5, entries 4 and 5, and Table 8, entries 10 and 11. This is in accord with the weak directing effect of the substituent on the diene (see (2) above), which enhances the importance of the detailed structure of the nitroso compound.

(4) Substituent effects are approximately additive.

The results of these studies are summarized in Table 9. This indicates the regiochemical outcome expected for each type of substituent on the diene. Z is a  $\pi$ -electron-withdrawing group and D a donor group. The letters indicate the degree to which this isomer is expected to be favored (large, medium, or small preference) and refer

(17) Labaziewicz, H.; Riddell, F. G. *J. Chem. Soc., Perkin Trans. 1* **1979**, 2926–2929.

(18) Häussinger, P.; Kresze, G. *Tetrahedron* **1978**, *34*, 689–696.

(19) Taylor, E. C.; McDaniel, K.; Skotnicki, J. S. *J. Org. Chem.* **1984**, *49*, 2500–2501.

(20) Sasaki, T.; Eguchi, S.; Ishii, T.; Yamada, H. *J. Org. Chem.* **1970**, *35*, 4273–4275.

(21) Ensley, H. E.; Mahadevan, S. *Tetrahedron Lett.* **1989**, 3255–3258.

(22) Houk, K. N.; Sims, J.; Duke, R. E., Jr.; Strozier, R. W.; George, J. K. *J. Am. Chem. Soc.* **1973**, *95*, 7287–7301.

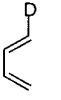
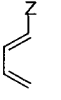
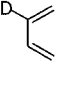
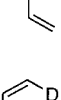
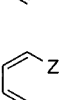
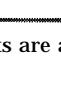
(23) Houk, K. N. *Top. Curr. Chem.* **1979**, *79*, 2–40; see pp 29–30.

**Table 8. Some Experimental Regioselectivity Data for Nitroso Cycloadditions with Substituted Butadienes**

Entry	Diene	Nitroso	Major product	Product ratio	Ref.
1			proximal	100:0	2
2			proximal	58:42	2
3			proximal	58:42	3
4			proximal	100:0 <sup>a</sup>	17
5			proximal	100:0 <sup>b</sup>	18
6			proximal	100:0	2
7			distal	100:0 <sup>b</sup>	18
8			distal	52:48	3
9			proximal	>76:<24	19
10			distal	100:0	20
11			proximal	80:20	17
12		HNO	proximal	60:40	21
13			proximal	88:22	21
14			distal	70:30	17
15			distal	>95:<5	17
16			proximal	75:25	8

<sup>a</sup> R = Me or Ph. <sup>b</sup> R<sup>1</sup> = H, Me; R<sup>2</sup> = H, MeO; R<sup>3</sup> = H, Me, Cl.

**Table 9. Generalizations Concerning the Regioselectivity of the Hetero-Diels–Alder Reactions of Nitroso Compounds with Substituted Dienes<sup>a</sup>**

HNO, RNO or ArNO			RCONO		Examples	
Diene type	Favored isomer	Extent of preference	Favored isomer	Extent of preference	Table 5 entries	Table 9 entries
	proximal	M	proximal	L	1, 2	1 to 5
	proximal	L	proximal	L	3	6
	proximal	S	distal	M	4, 5	9 to 15
	distal	M	distal	S	6	16
	distal	S	-	-	9	-
	proximal	L	-	-	7, 8	7, 8

<sup>a</sup> Effects are approximately additive such that predictions for multiply substituted dienes may also be made.

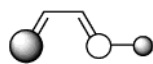
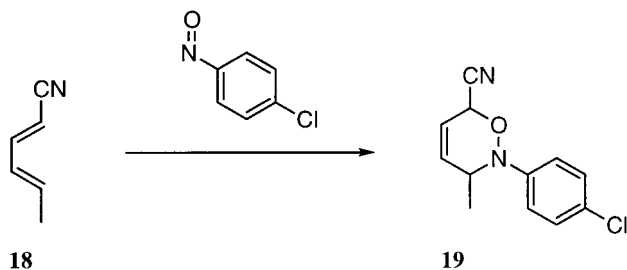


**Figure 4.** Qualitative form of the HOMO of each of the *trans*-1-substituted dienes studied.

**Scheme 7. Reaction of *p*-Chloronitrosobenzene with a Disubstituted Diene**



to the relevant table entries for theoretical and experimental data. Table 9 should allow predictions to be made about the regiochemical outcome for previously untried dienes. It makes correct predictions for each of the cases we are aware of except when sterics are significant enough to override the normal preferences (Table 8, entries 12 and 13).

Table 9, which uses the quantitative nature of our calculated regioselectivities, allows predictions about the cumulative effects of multiple substituents on a diene to be made. For instance, in Scheme 1, two very different substituents (and ester and an amine) give the same regioisomer with 100% selectivity. With our calculations

we can predict that when these two substituent types compete as in a 1,4-disubstituted diene, the ester would be most strongly directing, and consequently, the proximal isomer with respect to the ester would be preferred. Substituents whose particular directing effect has not been calculated but which fall into a particular class can also be subject to prediction.

### Conclusion

Hetero-Diels–Alder reactions of nitroso compounds are concerted but proceed through highly asynchronous transition states. Diradical and zwitterionic pathways only compete when nitroso compounds bearing a small nitrogen substituent react with dienes substituted with radical-stabilizing groups.

There is such a strong preference for the endo path that the exo may be expected to never be competitive; models designed to explain observed selectivities should be based on an endo transition state. The preference for the endo path arises from a combination of electrostatic repulsion between the lone pairs of RNO with the electron rich diene and also the repulsive interaction between the n-HOMO of the nitroso compound and the  $\pi$ -HOMO of the diene.

The regioselectivities of reactions of 1- and 2-substituted dienes involve the delicate balance of a number of interactions. Substitution at the 2-position of the diene generally has a smaller effect than at the 1-position. As a guide, the following substitution was found to favor the proximal isomer (in order): *cis*- or *trans*-1-CN >



*trans*-1-MeO > *trans*-1-Me. The following substitution was found to favor the distal isomer, again in order: 2-CN > 2-MeO > *cis*-1-Me. The remaining substituents (2-Me, *cis*-1-MeO) were found to have little influence either way.

The data presented will help put the prediction of the outcome of the Diels–Alder reactions of nitroso compounds on a sounder basis and aid in synthetic planning. Studies are underway to investigate the stereoselectivity of these reactions with chiral dienes and dienophiles.

**Acknowledgment.** We are grateful to Astra-Zeneca and the U.K. Fulbright commission for a fellowship to A.G.L. and to the National Institute of General Medical Sciences, National Institutes of Health, for financial support of this research. This work was partially supported by National Computational Science Alliance and utilized the NCSA HP/Convex Exemplar SPP-2000.

JO0104126